THE AMERICAN SOCIETY OF MECHANICAL ENGINEERS
345 E. 47th St., New York, N.Y. 10017

98-GT-496

3D RANS CALCULATIONS OF FLOW THROUGH TURBINE VOLUTES

R.G.M.Hasan and J.J.McGuirk
Department of Aeronautical and Automotive Engineering and Transport Studies
Loughborough University
Loughborough LE11 3TU
ENGLAND

ABSTRACT

Due to their complex shape and complicated flow configuration, the volutes of turbocharger compressors and turbines appear to be a difficult component for both numerical modelling and experimental measurements. This paper presents some 3-D Reynolds Averaged Navier-Stokes (RANS) calculations for a volute with a trapezoidal cross-sectional shape. Flow recirculation under the 'tongue' and treatment of radial outflow boundary condition are two important aspects of the current calculations. The results are compared with available experimental data and the reasons for the discrepancies are discussed. The flow features highlight the fact that very strong secondary velocities are present and hence the conventional one-dimensional analyses are not adequate for design purposes. The paper also highlights the typical problems faced by a numerical analyst from grid generation point of view and briefly describes a procedure for handling the problems. Generated grids for two different volutes are presented here in order to show the capability of the grid generation method.

NOMENCLATURE

A	Cross-sectional area
C_1, C_2, C_μ	Constants in turbulence model
G	Generation of turbulence
H	Depth of the trapezoidal volute at the throat
R_t	Radius of volute exit circle
TT	Thickness of the tongue at the 'throat'
WD	Volute exit width
Y	Normalised distance from volute wall to radial exit
k	Turbulent kinetic energy
p	Static pressure
r	Radial direction
S	Source terms
u, v, w	x, y, z components of the velocity vector
x, y, z	Cartesian coordinates

Greek Symbols

α	Flow angle measured wrt tangential direction
ε	Dissipation rate of turbulent kinetic energy
ρ	Density
μ	Viscosity
θ	Azimuth angle measured from throat

Subscripts

eff	Effective
i,j	Index
in	Inlet condition
k	Kinetic energy of turbulence
t	Turbulent
ε	Dissipation of turbulence
ϕ	General scalar variable

INTRODUCTION

The design of volutes or scrolls of small radial inflow turbocharger turbines is still based primarily on extremely simple assumptions such as one-dimensional inviscid flow (Watson and Janota, 1993). Such an approach, although very elementary, gives guidelines as to the overall area variation, flow angle at exit etc., but unfortunately it cannot capture local effects e.g., in the 'tongue' region (see Fig. 1) nor can it take into account the influence of alternative cross-sectional shapes, although an attempt to incorporate this parameter has been made by Owarish et al. (1992). In reality, the shapes of turbocharger volutes are usually very complex and often quite arbitrary. Because of this, the number of experimental and numerical studies is rather limited. This situation is further complicated by the interaction between rotor and volute flow and by the flow recirculation under the tongue. Most of the early works such as Hussain and Bhinder (1981), Khalil and Weber(1984) placed emphasis on flow properties near the exit radius (R_t in Fig. 1) of the volute in an attempt to understand the relationship between non-uniform exit flow properties and high fatigue stress on the impeller. One important conclusion made from these studies was that a clear understanding of the flow behaviour inside the scroll is an essential requirement in controlling such non-uniformities. It is only during the past decade or so that a few papers have appeared which address the volute flow patterns in more detail e.g., Tindal et al. (1987), Ayder and van den Braembussche (1994), Lobo and Elder (1993), Malak et al. (1987), Martinez-Botas et al. (1996) and Shyy and Vu (1991). The

Presented at the International Gas Turbine & Aeroengine Congress & Exhibition
Stockholm, Sweden — June 2–June 5, 1998

last two papers highlight the fact that the treatment of the radial exit boundary condition and handling of flow recirculation under the tongue are of utmost importance for successful and realistic numerical prediction of volute flow. Another important problem faced by the numerical analyst is the uncertainty about the three-dimensional geometry. It is apparent in the open literature that information about volute geometries is provided in the form of cross-sectional shapes at only a few selected azimuthal positions (e.g., Lobo and Elder 1993; Malak et al. 1987), often due to the proprietary nature of the volutes. This leads to difficult problem of generating an accurate representative of the complex geometry from limited data.

In this paper, we report some calculations on the flow inside a

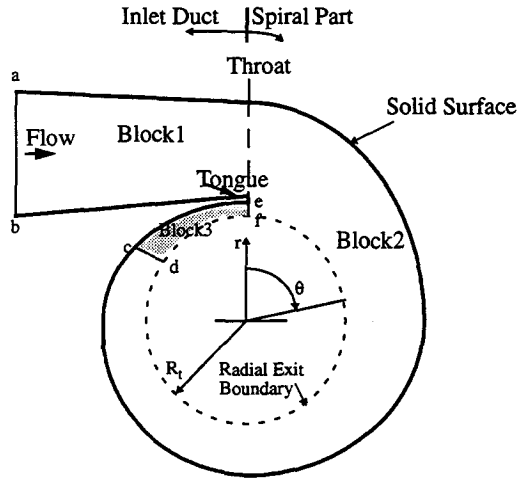

FIGURE 1: A Sketch of the Volute

trapezoidal volute whose geometrical information may be found in detail in Tindal et al. (1987) and Scrimshaw (1981). The reason for selecting this volute for prediction is to make sure that the geometrical uncertainties are completely removed, since it has been shown by others, e.g., Malak et al. (1987) that the flow field inside a volute is very sensitive to geometrical variation. Also, this choice of volute provides experimental and numerical data by other authors (Tindal et al., 1987, Hasan, 1990) at critical flow sections which will be compared with the current predictions.

GOVERNING EQUATIONS AND NUMERICAL PROCEDURE

The three-dimensional Reynolds-Averaged Navier-Stokes (RANS) equations along with a k-ε two-equation turbulence model are solved in the present study. For incompressible, steady-state flow the governing equations of mass continuity, momentum, k and ε are:

Continuity : $$\frac{\partial}{\partial x_j}(\rho u_j) = 0$$

Momentum: $$\frac{\partial}{\partial x_j}(\rho u_i u_j) = -\frac{\partial p}{\partial x_j} + \frac{\partial}{\partial x_j}\left\{\mu_{eff}\left(\frac{\partial u_i}{\partial x_j} + \frac{\partial u_j}{\partial x_i}\right)\right\}$$

Turbulence quantities: (ϕ = k, ε) $$\frac{\partial}{\partial x_j}(\rho u_j \phi) = \frac{\partial}{\partial x_j}\left\{\frac{\mu_{eff}}{\sigma_\phi}\left(\frac{\partial \phi}{\partial x_j}\right)\right\} + S_\phi$$

where,

$$S_k = (G - \rho\varepsilon)$$

$$S_\varepsilon = C_1 G - C_2 \rho \frac{\varepsilon^2}{k}$$

$$G = \left[\mu_t\left(\frac{\partial u_i}{\partial x_j} + \frac{\partial u_j}{\partial x_i}\right)\right]\frac{\partial u_i}{\partial x_j}$$

$$\mu_{eff} = \mu + \mu_t$$

$$\mu_t = C_\mu \rho\left(k^2/\varepsilon\right)$$

$$C_\mu = 0.09; C_1 = 1.44; C_2 = 1.92; \sigma_k = 1.0; \sigma_\varepsilon = 1.3$$

The co-ordinates of the differential operators in the above equations were expressed in general non-orthogonal curvilinear co-ordinates. All the flow variables viz., u, v, w, p, k and ε were stored at the centre of the finite volumes. In order to prevent the checkerboard pressure-velocity decoupling for this non-staggered variable arrangement, the commonly used smoothing technique based on momentum interpolation (Rhie and Chow, 1983) has been adopted in the program. Second order central differencing has been used for all terms except the convection terms which are approximated by the first-order 'hybrid' differencing scheme. The discretised equations were solved using the SIMPLE pressure correction method of Patankar and Spalding (1972).

The computer program is written for a structured mesh. Moreover, instead of the more popular direct addressing data structure, we have used an indirect addressing method to implement a simple technique of accommodating multiple blocks in the solution domain. This has allowed a simple multi-block treatment of the tongue region of the volute. This is briefly explained with reference to the two-dimensional step flow geometry as shown in Fig. 2. In a conventional approach, simple grids would be generated over the rectangular space abhdefg and the cells in the region bhdc blocked to create the step geometry. The computational cells are usually directly addressed viz., in the increasing i-direction (as shown in region bhdc) consecutive cells are numbered as (i-1,j), (i,j), (i+1,j) and similarly for other directions. In the current computer program, the flow field is considered to be made up of two blocks, Block1 and Block2. Suitable grids are then generated separately over these blocks such that the grid continuity at the interface cg is maintained. Obviously, the direct addressing technique is no longer workable. To avoid this problem and at the same time to maintain the advantages of simple grids, we have identified each cell (including the boundary elements which may be considered as zero thickness cells), by unique numbers such as I0, I1, I2, I3. etc. An additional array is then required in the program which stores the connectivity information identifying the neighbours of each cell. The use of the above addressing technique does not require any cell blocking but at the same time enables simple grids to be generated over individual

blocks. The only additional computer overhead is that of an extra connectivity array which stores information about cell neighbours. However, this is compensated for by the advantages mentioned above.

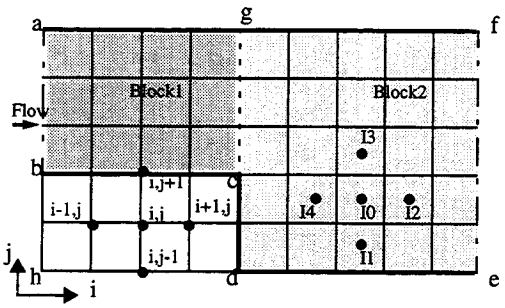

FIGURE 2: Illustration of cell addressing

GRID GENERATION

Considerable attention has been paid in the present work to the question of generating high quality grids inside the volute region, since this has been of some concern in previous work (e.g., Lobo and Elder, 1993). As shown in Fig. 1, a typical volute is made up of two sections, the inlet duct and the spiral part with the junction between them commonly known as the 'throat'. Generating a three-dimensional geometry for an arbitrary shaped cross-section is often a difficult task, especially due to the practical limitation of the unavailability of the geometrical detail as mentioned before. A significant amount of effort was hence made in the current research program to address this issue. A grid generation package applicable to arbitrary volute shapes was developed for this purpose. The procedure is capable of generating three-dimensional curvilinear structured grids for all types of volutes including twin-entry ones. Complete details of the approach are described in a paper under preparation (Hasan and McGuirk, 1998), so only a brief summary is described here. The volute cross-sectional area, A vs. azimuth angle, θ is first obtained from the limited number of available (usually 4-6) cross-sectional shapes. An iterative interpolation technique is then employed in order to obtain the cross-sectional shapes at all other azimuthal positions such that areas of the interpolated shapes conform to the design target A vs. θ curve. The individual cross-sections are then gridded by solving Poisson's equation along with standard smoothing techniques (Thompson, 1982). As an example of the application of the method, the single-entry volute referred to in Lobo and Elder (1993) has been considered. The cross-sectional shapes were provided at θ=0, 90, 180, 270 degrees. The generated geometry, grids and other features are shown in Fig. 3. The cross-section at the 'throat' (Fig. 3b) is divided into two areas: Area I represents the area at the end of the inlet duct and Area II represents the area at θ=360 deg through which the flow recirculates; TT represents the thickness of the tongue. The interpolated shapes between θ=270 and 360 degrees are shown in Fig. 3d and this shows the quality of the interpolated shapes obtained by the present procedure. It may be mentioned here that this volute represents 'sidewise' recirculating area rather than the more common 'under-the-tongue' recirculating' area as shown in the next example. The quality of grid shown in Fig. 3c is a substantial improvement on those shown in the first attempts of Lobo and Elder (1993).

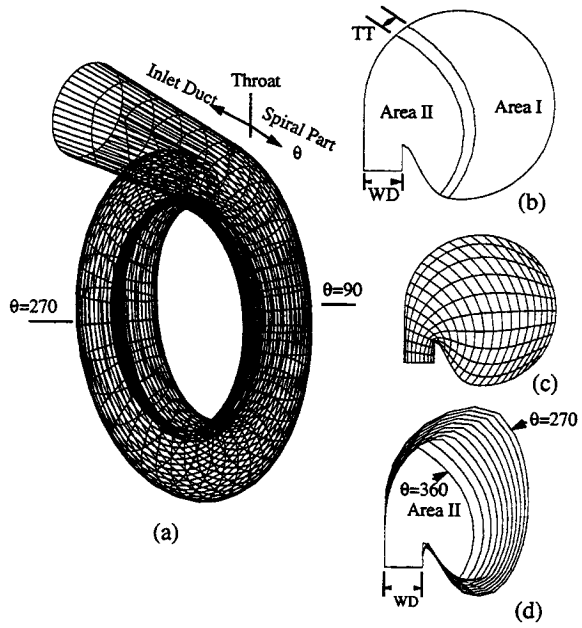

FIGURE 3: Arbitrary-shaped volute (Lobo, 1993)
(a) Wireframe, 46*21*11 grids
(b) Cross-section at throat (c) Cross-sectional grid
(d) Interpolated shapes between θ=270 to 360 deg

To indicate the flexibility of the method, figure 4 shows grids generated for a typical twin-entry volute. The shape of the inlet duct varies from rectangular to trapezoidal as shown in Fig. 4d. The quality of shape interpolation is obvious from this figure. Again the quality of grids generated in the volute cross-sections is high (Fig. 4c).

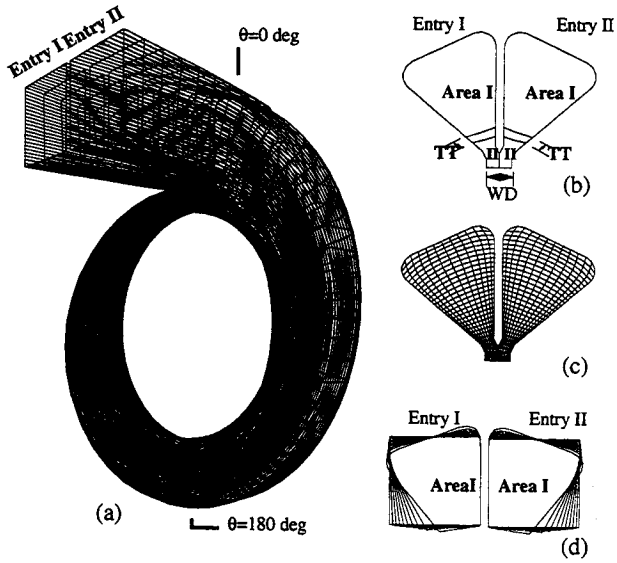

FIGURE 4: Twin-entry volute. (a) Wireframe (56*31*26)
(b) Cross-section at throat (c) Cross-sectional grid
(d) Interpolated shapes for Inlet Duct

Finally, the trapezoidal volute for which flow calculations are described below is considered. The geometrical detail was available in terms of cross-sectional dimensions (Scrimshaw, 1981) at a number of azimuthal positions. The cross-sectional area vs. θ curve is first drawn (which shows an almost linear variation for the most part) and then the current grid generation technique is applied. As before, the volute is made up of two sections but this time a 3-block grid approach is adopted; the first (Block1) is the inlet duct, the second (Block2) is the spiral section (θ=0 - 360 deg). Block3 is an overlapping curved section used for handling the recirculating flow under the tongue as explained below. Two different grids were generated, one coarse and uniform having 49*20*12 grid nodes and another fine and non-uniform having 93*40*24 grid nodes. A three-dimensional isometric view and a two-dimensional cross-sectional view of the finer grid are shown in Fig. 5a-b. Although a strict and systematic grid refinement procedure has not been followed, we believe from our previous experience (Hasan, 1990), that the fine grid is close enough to reveal the flow features in most regions of the domain accurately, at least for the type of results presented in this paper. Note also that the fine grid is approximately of double the density in each direction than that used by Martinez-Botas (1996) and Hasan (1997). One important point which needs highlighting here is that the cross-section of the volute (Fig. 5b) has been extended radially from the 'True Volute Exit' as defined in the experimental geometry (Scrimshaw, 1981) by a small distance towards the axis of the rotor in order to implement the current simple volute exit boundary conditions described below.

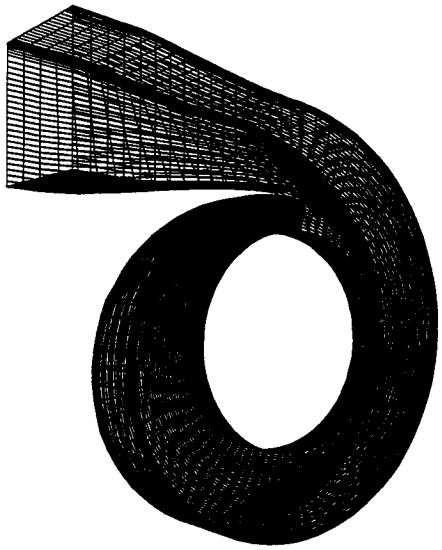

FIGURE 5a: 3D Grid for the Trapezoidal Volute (93 * 40 *24)

BOUNDARY CONDITIONS

At the inlet (plane ab, Fig. 1), the streamwise velocity has been specified from available experimental data. The distribution of turbulence intensity and its dissipation rate were given the following values

$$k_{in} = 0.001 W_{in}^{2} \text{ and } \varepsilon_{in} = k_{in}^{1.5} / (0.01H)$$

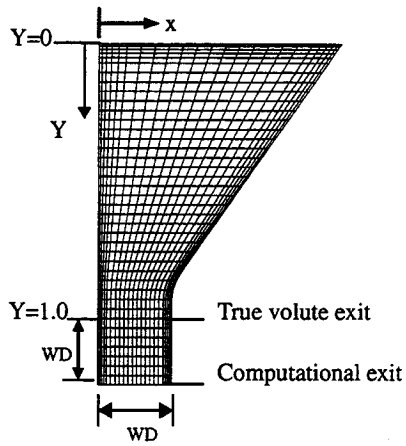

FIGURE 5b: Grid Distribution at a Cross-section (40*24)

where W_{in} is the inlet velocity and H is the volute depth (Depth between Y=0 to Y=1 in Fig. 5b) at the throat. For all solid surfaces, no-slip conditions were specified and standard high Reynolds number wall functions applied.

There is no obvious choice for the boundary condition at the radial exit plane. The strictly correct procedure, but certainly not the most efficient, would be to include the flow over the nozzle guide vanes (if present) and also the rotor blades as part of the volute calculation. Considerable computational expense can therefore be saved by adopting a simpler approach. Shyy and Vu (1991) describe a variable pressure loss method based on an estimate of the blockage and loss effects of the embedded aerofoils treated as a region of flow through a 'porous medium'. As indicated by Shyy and Vu (1991), this is not necessary if interest is focused on volute flow. Indeed, Tindal et al. (1987) demonstrate that rotor removal had little effect on the shape of volute velocity profiles.Lobo and Elder (1993) have used constant static pressure, Martinez-Botas et al. (1996) have used experimental values and Khalil and Weber (1984) have used 'rotor simulator' condition, other details of this were not provided. At present no attempt has been made to implement a rotor simulation type of boundary condition. It is believed that a simpler exit condition is sufficient for many volute analysis purposes. A comparison has been made (Hasan and McGuirk, 1997) between a uniform exit V_r condition and a V_r which varies circumferentially depending on the local magnitude of the radial pressure gradient - little difference was observed, so uniform V_r has been chosen for the present predictions. However, to allow some 'extra' space for the flow to adjust to this simplified condition, the exit circle (radius R_t, Fig. 1) was reduced from the true volute exit value by distance 'WD' as shown in Fig. 5b. The selection of the above extension length was as follows. Too small a value would affect the results near the true exit because of the 'approximate' nature of the boundary condition and too high a value would 'change' the overall geometry. A compromise was found after making a few initial runs and the extension was taken to be equal to WD. For all variables except the radial exit velocity V_r, a zero gradient approximation was used at the computational exit. The radial exit velocity V_r was given a uniform value such that the total inflow mass is balanced. The assumption of uniform radial exit velocity is a very elementary simulation of the volute flow in the sense that the flow through the volute can be assumed to be a sink flow superimposed on a circumferential

motion. It is fully recognised that this treatment needs eventually to be replaced by a rotor simulation boundary condition.

Another boundary condition is required at plane ef in Fig. 5c

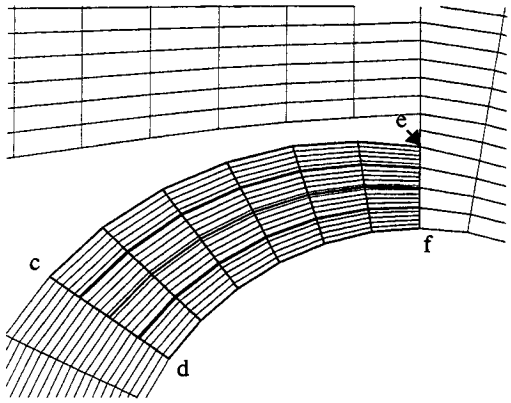

FIGURE 5c: Tongue Region Blow-up on a Coarse Grid

(under the 'tongue', Fig. 1). The situation here is complicated by the fact that although this is effectively the topological 'exit' of the computational domain, a small amount of flow crosses this boundary and within the multi-block topology rejoins the stream of fluid coming from the inlet duct. Martinez-Botas et al. (1996) have stated that a cyclic boundary condition was used on this boundary, but it is not clear how this can be done for a single block structured mesh when the number of cells in adjacent planes (on two sides of plane ef) are different. To handle this within the current mesh, we have included a third block cdfec as shown in Fig. 5c which overlaps the last 60-degrees of block2 and a coarse mesh (shown by thicker lines in the tongue region blow-up) has been generated in this third block such that the block 3 grid matches exactly with the portion of the block 2 grid below the tongue at location ef. Fixed boundary conditions are then specified at planes cd (of block 3) and ef (of block 2). The boundary values at plane cd (of block 3) are updated by interpolation from the field values calculated at plane cd (of block 2) in the previous iteration, while the boundary values at plane ef (of block 2) are fixed by interpolating from the field values at plane ef (of block 3). In actual calculations, the updating of values is done every 10 iterations and the solution is declared converged when the field values become insensitive to further iterations. It may be mentioned that Lobo and Elder (1993) have also reported a similar procedure for the handling of recirculating flow under the tongue.

CALCULATION DETAILS

Calculations were carried out on a SUN SPARC-10 Work Station and a total of 1200 iterations were necessary for the calculation which took about 16 hours of CPU. The addition of block 3 in the calculation represents a small overhead and adds only 2.7% of extra grid nodes.

RESULTS AND DISCUSSION

Development of the Flow

Figure 6a shows the predicted velocity vectors on an azimuthal plane (A-A) and Figs. 6b-e show the vectors on four cross-sectional planes. The azimuthal velocity accelerates in the inlet duct and for most of the spiral section it demonstrates a free-vortex-like pattern. The effect of the radial pressure gradient can be clearly seen from the strong secondary velocity vectors. Although the secondary velocity is much stronger near the side walls and less in the core regions, similar to conventional curved duct flows (Berger et al., 1983), the typical streamwise vortical motion is almost absent. However, in the middle region of the volute (see Figs. 6c-d) there is a tendency for a vortex to begin to form near the top wall of the cross-section. This particular feature of volute flow development is more likely to be due to the large radial acceleration rather than the particular (trapezoidal) volute shape. Calculations on a circular shaped volute (Martinez-Botas et al., 1996) also do not show any vortical motion. In the vicinity of the tongue both the azimuthal and the secondary velocities (θ=2.4 deg) are smaller due to the combined effect of 'sudden expansion' and flow recirculation.

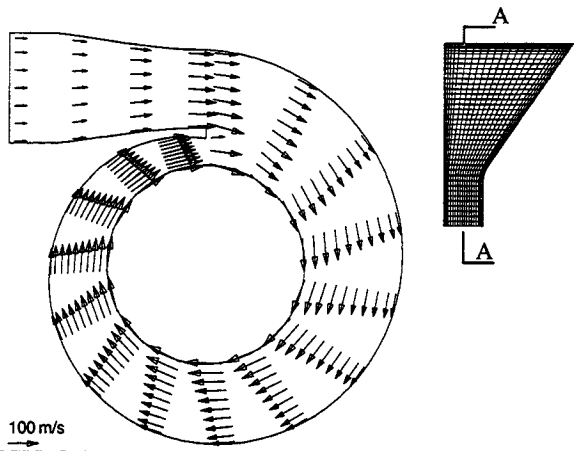

FIGURE 6a: Velocity Vector on an Azimuth Plane A-A

The streamwise (azimuthal) velocities at two cross-sectional planes are compared with available experimental, numerical and theoretical data in Figs. 7a-b. These profiles are plotted on the plane AA indicated in Fig. 6a and use the non-dimensional distance from the outer volute wall Y (Fig. 5b) as parameter. At this θ plane, apart from a boundary layer found on the outer wall, the profile follows a free-vortex shape quite closely (although at a higher velocity than implied by the theoretical free-vortex velocity) until the tongue region is reached. The improvement of results due to the current tongue and flow recirculation treatment can be clearly seen in Fig. 7a. The numerical work of Hasan (1990), used a coarser mesh and did not consider any recirculation. The deviation of the present result from experimental data near the volute exit (Y ~ 1.0) can be partly attributed to the 'artificial' geometrical extension of the volute exit as mentioned before but also to mesh coarseness in the near-tongue region; the profile shape could probably be improved with further local mesh refinement. The comparison of velocity at θ=180 deg also shows excellent agreement with experimental data. The theoretical free vortex velocity profile again shows reasonable agreement with experiments at θ=180 deg but discrepancy between theory and experiment is observed near the outer wall due to the boundary layer effects. These observations clearly demonstrate the need for a 3D viscous design procedure.

The static pressure contours at two cross-sections are shown in Figs. 8a-b. Because of the simple cross-sectional geometry, the

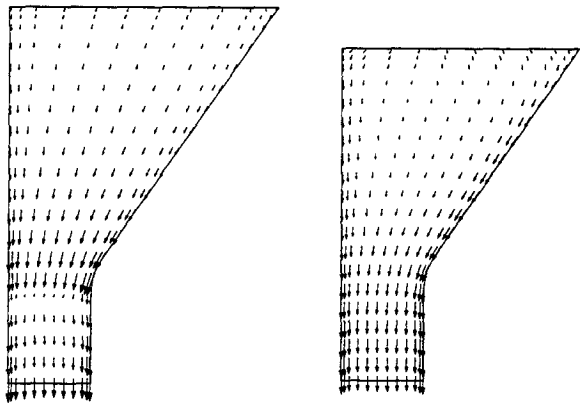

(b) θ=2.4 deg (c) θ=90 deg

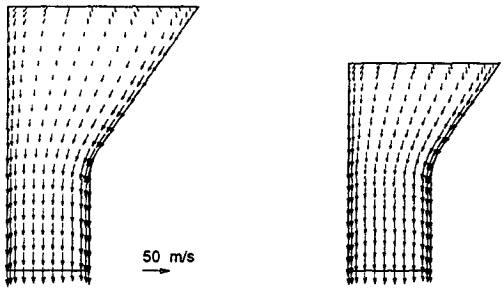

(d) θ=180 deg (e) θ=270 deg

FIGURE 6b-e: Development of Secondary Velocity

contours are rather uniformly spaced and this supports the fact that a free-vortex design procedure may yield generally acceptable agreement for the most part of the spiral section.

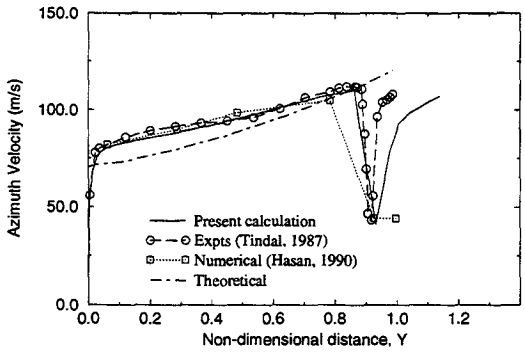

FIGURE 7a: Comparison of Azimuth Velocity at θ=2.4 deg

Flow Angle

A comparison of the exit flow angle (measured on plane A-A with respect to the tangent at the true volute exit boundary) with other available data is made in Fig. 9. Flow angle is predicted signif-

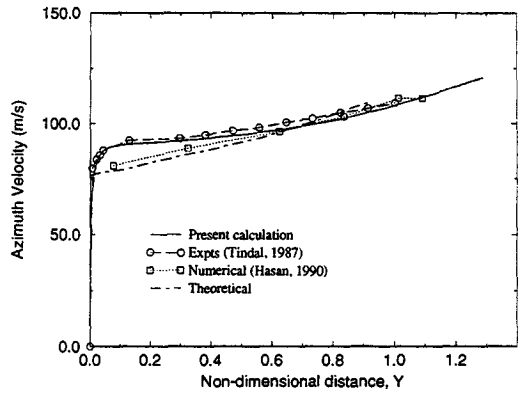

FIGURE 7b: Comparison of Azimuth Velocity at θ=180 deg

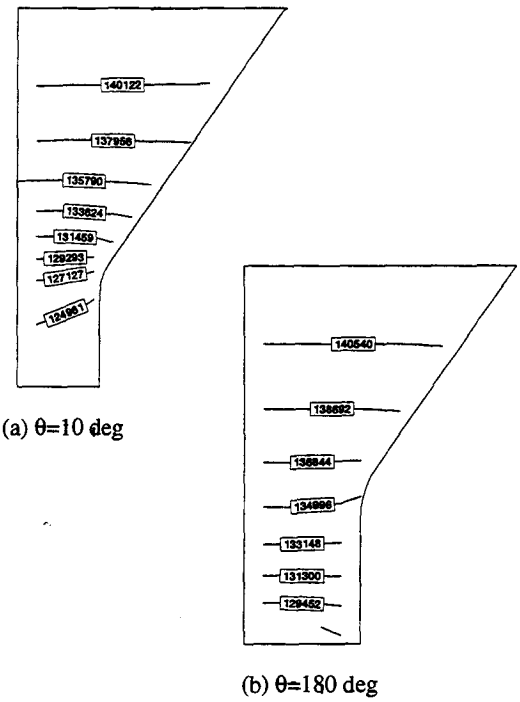

(a) θ=10 deg (b) θ=180 deg

FIGURE 8a-b: Static Pressure Contours at Different Cross-sections

icantly better in the present predictions compared with Hasan (1990). This is particularly so in the tongue region near 0 and 360 deg where the previous predictions (which did not allow 'carry-over') indicated a wrong trend. The main cause of the improvement is the introduction of the tongue/ recirculation treatment rather than the grid resolution. Part of the discrepancy may be attributed to the approximate treatment of rotor-volute interaction. For example, with V_r specified as constant and positive, it is not possible to predict negative flow angles as observed very close to the tongue region. Apart from this problem, however, the current method reproduces the shape of the flow angle curve very well. The theoretical free-vortex result cannot pick up the flow angle variations because of its inherent limitations. Flow angle contours at two locations are shown in

Fig. 10a-b. The effect of the tongue and recirculation can be seen in high flow angle values in the initial region as in Fig. 10a. It can also be noted that the flow angle varies considerably in the azimuthal direction across the volute exit, so that an analysis based on the present approach is certainly necessary to provide adequate information for design of nozzle vanes or to assess incidence angles onto the turbocharger blades.

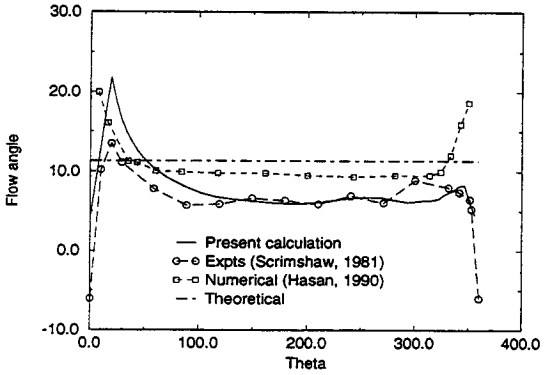

FIGURE 9: Flow Angle Variation at Volute Exit Radius

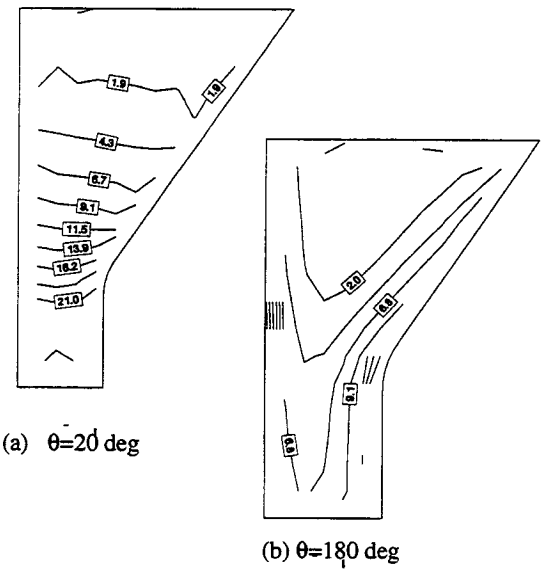

(a) θ=20 deg

(b) θ=180 deg

FIGURE 10a-b: Flow angle variation at two cross-sections

Flow Field Near the Tongue

The 'tongue' represents the most difficult region from the design point of view. In the current calculation procedure, the tongue has been accommodated by considering a third computational domain as mentioned before. Some simplification of the actual smooth shape has also been made. This is not a limitation of the present grid generation approach but rather a choice we have made to minimise the mesh size to that which is sufficient to capture the tongue effects without necessarily resolving every geometrical detail, as shown in Figs. 7 and 9, the present tongue shape approximation seems quite acceptable. The predicted static pressure and flow angle distribution in the tongue region are shown in figures 11and 12. The axial (x-direction in Fig. 5b) location of these planes is again on AA as shown in Fig. 6a. Significant pressure and flow angle variations can be seen in these plots. Figure 12 shows how the uniform rectilinear flow coming from the inlet duct undergoes sudden expansion and mixes with the recirculating flow resulting in a distorted flowfield in the vicinity of the tongue. Information of the large pressure gradients and flow angle in this region is undoubtedly of value in design considerations of volute rotor interactions.

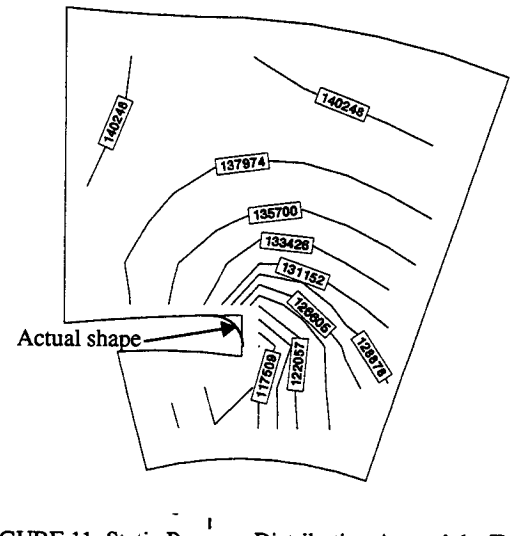

FIGURE 11: Static Pressure Distribution Around the Tongue

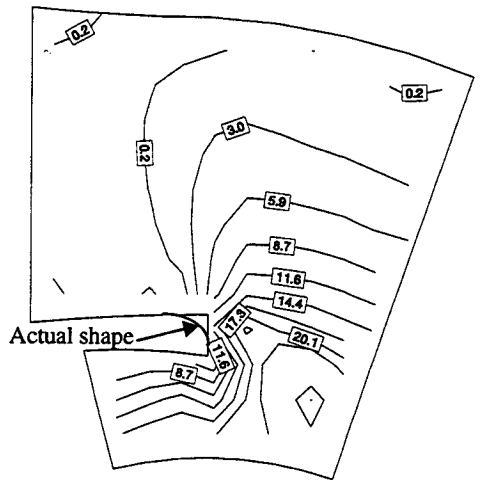

FIGURE 12: Flow Angle Distribution Around the Tongue

CONCLUDING REMARKS

The research described in this paper clearly indicates that the present approach to the handling of flow inside volutes is a practical

one. The results obtained by using the current methodology can be of great significance to designers and engineers working on turbomachinery components. The present study also emphasises the fact that more critical experimental data along with precise information about geometries are necessary for validation purpose. The conclusions and recommendations may be summarised as follows:

A. The presence of strong secondary velocities indicate the need for a fully three-dimensional design approach. Of the two critical volute specific boundary treatments viz., flow recirculation under the tongue and accurate specification of condition at the radial exit, the former has been successfully implemented in the current method. However, more work is necessary in order to find alternative treatments for the simple approach adopted for the latter. One method would be to use the volute-rotor system as one unit and thus remove the necessity of a boundary condition altogether. However, the feasibility of such an approach for practical use is a matter of serious concern because of the requirement of very high computing resources. A preferred route would be to simulate the boundary condition at the radial exit by adopting the idea of 'Actuator Disc' (Tuffrey et al., 1996, Joo W-G, 1994), where the presence of rotor and/or nozzle can be approximated by applying a set of jump condition on two sides of a zero-thickness cell. Very briefly, a total of five physical constraints are to be satisfied: three of which are the conservation principles for mass, momentum and rothalpy; the other two are the specification of blade angle at exit from the rotor and the rotor output. Work is underway in order to examine the effects of this approach.

B. The one-dimensional free-vortex approach may provide elementary guidelines for some regions of the flow, but it completely fails to provide any useful results near the tongue region.

C. Even with the present simple boundary condition approximations, good simulation of flow field including the effects of tongue flow is possible, and data on local flow angle and pressure variations of value to turbocharger blade design can be obtained.

ACKNOWLEDGEMENTS

The authors are grateful to the UK Engineering and Physical Sciences Research Council for the award of a grant to support (GR/J11652) the above research.

REFERENCES

Ayder E., Van den Braembussche R.A.,1994, 'Numerical Analysis of the Three-dimensional Swirling Flow in Centrifugal Compressor Volutes', ASME J. of Turbomachinery, Vol. 116, No. 3, pp. 462-468.

Berger S.A., Talbot L., Yao L.-S., 1983, 'Flow in Curved Pipes', Annual Review of Fluid Mechanics, Vol. 15, pp. 461.

Hasan R.G.M.,1990,Numerical Prediction of Flow in Curved Ducts and Volute Casings',PhD Thesis, University of London.

Hasan R.G.M., McGuirk J.J., 1997, '3D Viscous Calculations of Flow Through a Single-entry Turbocharger Turbine Volute', Paper to be presented at the 7th Asian Congress of Fluid Mechanics, Dec. 8-12, Madras, India.

Hasan R.G.M., McGuirk J.J., 1998, 'Simple and Flexible Gridding Method for CFD Analysis of Volute Flows' (in preparation).

Hussain M., Bhinder F.S.,1984, 'Experimental Study of the Performance of Nozzle-less Volute Casing for Turbocharger Turbines', SAE Paper No.840571.

Joo W-G, 1994, Intake/engine Flowfield Coupling in Turbofan Engines, PhD Thesis, Cambridge University.

Khalil I.M. and Weber H.G., 1984, 'Modelling of 3DFlow in Turning Channels', ASME J. of Eng. for Power, Vol. 106, No.3.

Little A.R, Manners A.P., 1993, 'Predictions of the Pressure losses in 2D and 3DModel Dump Diffusers', ASME Paper 93-GT-184

Lobo M., Elder R.L.,1993, 'The Modeling of Flow in the Volute and Vanes of a High Pressure Radial Inflow Turbine', ASME Paper 93-GT-59.

Malak M.F., Hamed A., Tabakoff W,1987, 'Three-dimensional Flow Field Measurements in a Radial Inflow Turbine Scroll Using LDV', ASME J. of Turbomachinery, Vol. 109, No. 2, pp. 163-169.

Martinez-Botas R.F., Pullen K.R., Shi F.,1996, 'Numerical Calculations of a Turbine Volute Using a 3-D Navier-Stokes Solver', ASME Paper 96-GT-66.

Owarish H.O., Ilyas M., Bhinder F. S., 1992, 'Two-dimensional Flow Analysis Model for Designing a Nozzle-less Volute Casing for Radial Flow Gas Turbines', ASME J. of Turbomachinery, Vol. 114, No. 2, pp. 402-410.

Patankar S.V., and Spalding D.B., 1972, 'A Calculation Procedure for Heat, Mass and Momentum Transfer in Three-Dimensional Parabolic Flows', Int. J. Heat and Mass Transfer, Vol. 15, pp. 1787.

Rhie C.M., and Chow W.L., 1983, 'A Numerical Study of the Turbulent Flow Past as Isolated Airfoil', AIAA J., Vol. 21, No. 11, pp.1525-1532.

Scrimshaw K.H., 1981, Scale Effects in Small Geometrically Similar Radial Gas Turbines with Particular Reference to Blade-less Volute Phenomena, PhD Thesis, University of London.

Shyy W., Vu T. C., 1991, 'Modelling and Computation of Flow in a Passage With 360-deg Turning and Multiple Aerfoils', ASME J. Fluids Eng., Vol. 115, pp.103-108.

Tindal M. J., Williams T. J., Khalil A. I., 1987, 'Flow in the Volutes of Small Radial Turbines', ASME Paper 87-ICE-48.

Thompson J.F., 1982, Numerical Grid Generation, North Holland, New York.

Tuffrey J., Kingston T.R., Hercock R.G., 1996, 'Efficient Modelling of Engine/Installation Interaction', Proceedings of the Engine-Airframe Integration Conference, Royal Aeronautical Society, UK, ISBN 1 85768 092 8.

Watson and Janota,1993, 'Turbocharging the Internal Combustion Engine',MacMillan Press.